Scale Setting for CLS 2+1 Simulations

Ben Straßberger,[a,*] **Marco Cè,**[f] **Sara Collins,**[c] **Antoine Gérardin,**[g] **Georg von Hippel,**[b] **Piotr Korcyl,**[e] **Tomasz Korzec,**[d] **Daniel Mohler,**[h] **Andreas Risch,**[a] **Stefan Schaefer,**[a] **Wolfgang Söldner**[c] **and Rainer Sommer**[a]

[a] *John von Neumann Institute for Computing (NIC), Deutsches Elektronen-Synchrotron DESY,*
Platanenallee 6, 15738 Zeuthen, Germany

[b] *Johannes Gutenberg-Universität Mainz*
Johann-Joachim-Becher Weg 45, 55099 Mainz, Germany

[c] *Institut für Theoretische Physik, Universität Regensburg,*
Universitätsstraße 31, 93040 Regensburg, Germany

[d] *Bergische Universität Wuppertal,*
Gaußstraße 20, 42119 Wuppertal, Germany

[e] *Institute of Theoretical Physics, Jagiellonian University,*
ul. Gołębia 24, 31-007 Kraków, Poland

[f] *Department of Theoretical Physics, CERN,*
1211 Geneva 23, Switzerland

[g] *Centre de Physique Théorique, Campus of Luminy,*
Case 907, F-13288 Marseille cedex 9, France

[h] *Helmholtzzentrum für Schwerionenforschung (GSI),*
Planckstrasse 1, 64291 Darmstadt, Germany

E-mail: ben.strassberger@desy.de, stefan.schaefer@desy.de

We present an update of the scale setting for $N_f = 2 + 1$ flavor QCD using gradient flow scales and pseudo-scalar decay constants. We analyze the latest ensembles with $2 + 1$ flavors of non-perturbatively improved Wilson fermions generated by CLS for improved precision. Special care is taken to correct for mistuning by measuring directly the mass derivatives of the various observables. We determine t_0 with input taken from a combination of leptonic decay rates of the Pion and the Kaon.

The 38th International Symposium on Lattice Field Theory, LATTICE2021 26th-30th July, 2021
Zoom/Gather@Massachusetts Institute of Technology

*Speaker

1. Introduction

CLS is a consortium which has generated a set of gauge field configurations with non-perturbatively improved Wilson fermions [1, 2]. One of the basic tasks in such an endeavor is the determination of the lattice spacing. Since the initial analysis of the scale for the CLS $2 + 1$ flavor ensembles [3], a much larger dataset has become available.

In this updated analysis, 20 ensembles with lattice spacings from 0.085 fm to 0.037 fm and Pion masses from 430 MeV to 134 MeV are included. The scale is set using a combination of Pion and Kaon decay constants and the flow scale t_0 [4] as an intermediate scale. The value of this intermediate scale in physical units is relevant for the precision determination of α_s [5], the η and η' masses and decay constants [6], moments of distribution amplitudes [7, 8], nucleon axial form factors [9], the proton radius [10], the Muon magnetic moment [11], and more.

As an improvement with respect to the previous analysis, we also include the reweighting factors originating from the negative sign of the strange quark determinant [12], which occur on a small subset of the gauge field configurations.

Our ensembles have been generated along a line of constant sum of the bare quark masses $\mathrm{tr}(M) = m_u + m_d + m_s = \mathrm{const}$. For each coupling, this sum has been tuned such that this line approximately passes through the point of physical light and strange mass. Of course, the precise value of this is only known after the analysis has been completed. We therefore have to deal with a certain amount of mistuning, for which we use the same method as in the previous analysis, i.e. by computing the derivatives of our observables with respect to the quark masses.

We measure two-point correlators and extract the pseudo-scalar mass, m_{PS}, and decay constant, f_{PS}, for the Pion and the Kaon as well as the PCAC mass, m_{PCAC}, for the corresponding quark combinations. The extraction of these quantities is done using plateau averages and fits as laid out in [3]. The gradient flow scale t_0 is defined by the clover definition of the action density and the Wilson flow [4]. Its improved definition [13] was not yet available when the simulations were planned. The measurements are then subjected to the next-to-leading order χPT finite volume correction according to [14]. The finite volume correction does not exceed the statistical error of the respective quantities. We nevertheless include 50% of the correction as an additional uncertainty.

From these measurements we calculate the dimensionless quantities,

$$\phi_2 = 8t_0\, m_\pi^2, \quad \phi_4 = 8t_0\left(m_K^2 + \frac{1}{2}m_\pi^2\right), \tag{1}$$

$$\sqrt{t_0}f_{\pi K} = \sqrt{t_0}\frac{2}{3}\left(f_K + \frac{1}{2}f_\pi\right). \tag{2}$$

The combination of Pion and Kaon decay constants $f_{\pi K}$ will be used to set the scale. ϕ_2 and ϕ_4 will form the basis of the analysis since in lowest order χPT $\phi_2 \propto m_u + m_d$ and $\phi_4 \propto m_u + m_d + m_s$.

In our analysis, we define lines of constant physics by setting ϕ_4 to a certain value. We use ϕ_4, because it is non perturbatively improved up to order a^2 along the CLS quark-mass trajectory.

We therefore proceed with the following steps: by measuring $\sqrt{t_0}f_{\pi K}$ and its mass derivatives on each ensemble, we can predict $\sqrt{t_0}f_{\pi K}$ at given values of ϕ_4, ϕ_2. The chiral behavior of this data can now be fitted and taken to the continuum. By tuning ϕ_4 such that the continuum curve passes through the physical point, we can then determine the physical value of t_0 and the lattice spacing at which we had done the simulations.
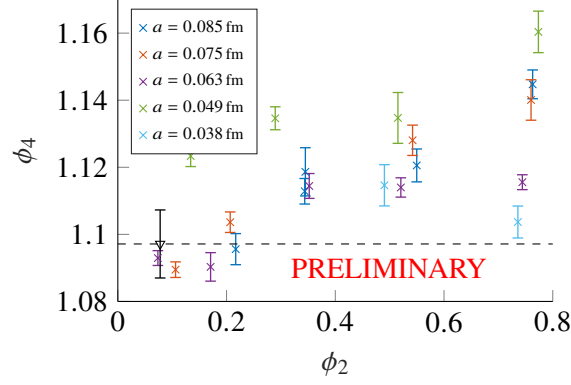
2

Figure 1: Measurements for ϕ_4 show the mistuning in ϕ_4 = const. The physical point, as calculated by this analysis, is shown as a triangle.

2. Observables at physical ϕ_4

Since the ensembles lie on a line of constant sum of the bare quark masses, more precisely $2/\kappa_l + 1/\kappa_s$ = const, the condition ϕ_4 = const is certainly not fulfilled for all ensembles due to discretization effects and higher order effects in χPT . On top of that comes the fact that the physical ϕ_4 has not been known during the planning of the simulations — and also depends on the particular discretization chosen for t_0. In fig. 1, we present our ensembles in the ϕ_2–ϕ_4 plane and observe that the sum of the three quark masses is within 8% of the physical value.

To get the observables at a given value of ϕ_4, we measured the derivatives $\frac{dX}{dm_i}$ of the observables X with respect to the quark masses of all the involved measurements. With these we can construct the derivatives with respect to ϕ_4,

$$\frac{dX}{d\phi_4} = \sum_{i=1}^{3} n_i \frac{dX}{dm_i} \bigg/ \left(\sum_{i=1}^{3} n_i \frac{d\phi_4}{dm_i} \right). \tag{3}$$

Here $\vec{n}$ is the direction of the shift in the space of quark masses. It has an effect on distance of the shift needed to reach the given value of ϕ_4 and thus on the resulting uncertainty. For the symmetric ensembles we use $\vec{n} = (1, 1, 1)/\sqrt{3}$ to preserve the symmetry and which was also the choice in [3]. For other ensembles, however, we use the direction $\vec{n} = (0, 0, 1)$, which we found to be close to optimal, in the sense that it minimizes the errors of the shifted values of $f_{\pi K}$. Since the shifts are typically less than 5% in the sum of the quark masses, we do expect the leading order of the Taylor expansion to give results with a systematic error below our statistical uncertainty. This also has been verified with a few ensembles at the symmetric line at a different sum of quark masses.

In the 2016 analysis [3], we shifted the results on each ensemble individually. In our update, we now model the mass derivatives of the observables as a function of quark mass and lattice spacing. This makes the predictions more stable and also allows the use of ensembles, where the derivatives have not been measured. With these derivatives the measurements can now be shifted to the desired ϕ_4 by

$$X(\phi_4^{\text{phys}}) = X(\phi_4) + \frac{dX}{d\phi_4} \left(\phi_4^{\text{phys}} - \phi_4 \right). \tag{4}$$

3. Chiral and Continuum Extrapolation

In the description of the analysis, we now have data at any given value of ϕ_4, which is a proxy for the sum of the two degenerate light and strange quark masses. To get to the physical point, we need to describe its chiral behavior and extrapolate to physical light quark masses given by ϕ_2^{phys}.

Chiral perturbation theory [15, 16] predicts

$$f_{\pi K} = f \left[1 - \frac{7}{6} L \left(\frac{\phi_2}{\bar{F}^2} \right) - \frac{4}{3} L \left(\frac{\phi_4 - \frac{1}{2}\phi_2}{\bar{F}^2} \right) - \frac{1}{2} L \left(\frac{\frac{4}{3}\phi_4 - \phi_2}{\bar{F}^2} \right) + k\phi_4 + O\left(M^2 \right) \right] \tag{5}$$

for the quark mass dependence of $f_{\pi K}$ in terms of a single SU(3) χPT NLO low energy constant, $k \propto (L_5 + 3L_4)$ as well as

$$L(x) = x \log(x), \quad \bar{F} = 4\pi \sqrt{8t_0} \, f. \tag{6}$$

We defined $\bar{F}$ in terms of f, the decay constant in the chiral limit. We then use a fit function for the chiral and continuum[1] behavior

$$F_\chi(\phi_2, \phi_4) = F_\chi^{\text{cont}}(\phi_2, \phi_4) \cdot \left(1 + C \cdot \frac{a^2}{t_0} \right) \tag{7}$$

$$F_\chi^{\text{cont}}(\phi_2, \phi_4) = \frac{A}{8\pi\sqrt{2}} \left[1 - \frac{7}{6} L \left(\frac{\phi_2}{A^2} \right) - \frac{4}{3} L \left(\frac{\phi_4 - \frac{1}{2}\phi_2}{A^2} \right) - \frac{1}{2} L \left(\frac{\frac{4}{3}\phi_4 - \phi_2}{A^2} \right) + B\phi_4 \right] \tag{8}$$

with the parameters $A = A(\phi_4)$ and $B = B(\phi_4)$ for each fixed value of ϕ_4.

It is worthwhile to consider the ratio of the chiral function

$$\frac{F_\chi^{\text{cont}}(\phi_2, \phi_4)}{F_\chi^{\text{cont}}(\phi_2^{\text{sym}}, \phi_4)} = R_\chi(\phi_2, \phi_4) + O(M^2) \tag{9}$$

since

$$\begin{aligned} R_\chi(\phi_2, \phi_4) = 1 &- \frac{7}{6} L \left(\frac{\phi_2}{A^2} \right) - \frac{4}{3} L \left(\frac{\phi_4 - \frac{1}{2}\phi_2}{A^2} \right) - \frac{1}{2} L \left(\frac{\frac{4}{3}\phi_4 - \phi_2}{A^2} \right) \\ &+ \frac{7}{6} L \left(\frac{\phi_2^{\text{sym}}}{A^2} \right) + \frac{4}{3} L \left(\frac{\phi_4 - \frac{1}{2}\phi_2^{\text{sym}}}{A^2} \right) + \frac{1}{2} L \left(\frac{\frac{4}{3}\phi_4 - \phi_2^{\text{sym}}}{A^2} \right) \end{aligned} \tag{10}$$

is free of parameters in NLO χPT, except for a weak dependence on A in the logarithms. We observe no systematic deviations from NLO χPT as shown in fig. 2.

In the same spirit the discretization effects are illustrated in the right hand plot of the same figure. Dividing each data point by the continuum χPT formula eq. (8) we expect the ratio

$$R_{\text{cont}} = \frac{F_\chi(\phi_2, \phi_4)}{F_\chi^{\text{cont}}(\phi_2, \phi_4)} = 1 + C \cdot \frac{a^2}{t_0} \tag{11}$$

---

[1]We note that logarithmic corrections of the a^2 terms in the form $a^2 \alpha_s (1/a)^{\hat{\Gamma}}$ are present [17]. The known leading exponent $\hat{\Gamma}$ is reasonably small and in particular we here use the Gradient Flow observable t_0. In this case the leading $\hat{\Gamma}$ vanishes in the pure gauge theory [18] and is not yet known in full QCD. We therefore ignore the presence of the logarithmic corrections at present.
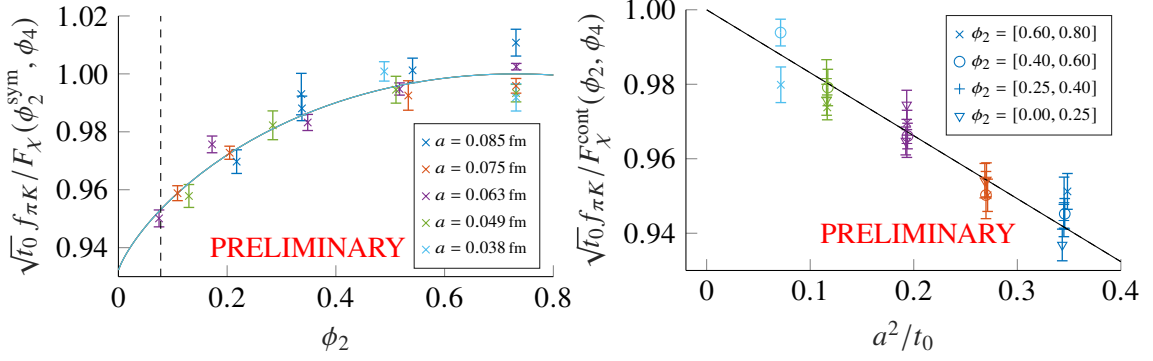
Figure 2: The chiral extrapolation on the left shows the measured data of $\sqrt{t_0}f_{\pi K}$ normalized by the fit function at the symmetric point. The solid line is the NLO χPT prediction, which does not depend on any NLO parameters and only logarithmically on the LO parameter A. No systematic deviation from this continuum formula can be detected. On the right, the continuum extrapolation of the same data, normalized by the fit-function evaluated for $a = 0$, is shown.
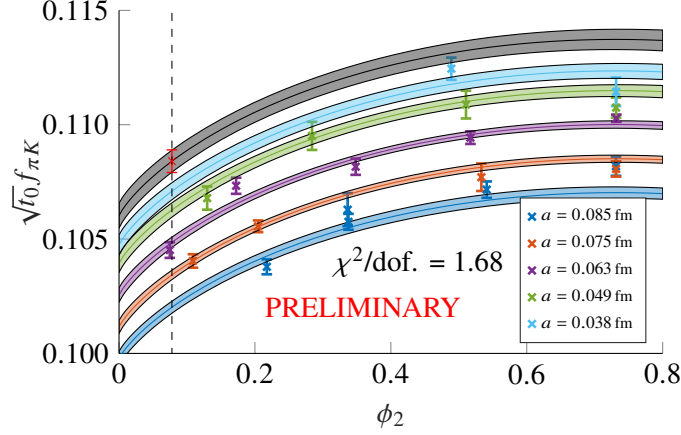

Figure 3: Chiral and Continuum Extrapolation of $\sqrt{t_0}f_{\pi K}$.

to be a linear function in a^2 to leading order of the Symanzik expansion. Again, no deviation due to higher order terms is detected.

These considerations confirm the fit function given in eq. (7), from which we extract the central value and statistical uncertainty of $\sqrt{t_0}f_{\pi K}$. This central fit is displayed in fig. 3. It takes into account the data of the ensembles with $a < 0.085$ fm. The stability when applying other cuts to the data is considered later.

The combined chiral and continuum extrapolation is now evaluated at ϕ_2^{phys} to determine $\sqrt{t_0}f_{\pi K}$ at the physical point. Together with the values [19, 20]

$$f_\pi^{\text{isoQCD}} = 130.56(02)(13)(02) \text{ MeV}, \quad f_K^{\text{isoQCD}} = 157.2(2)(2)(4) \text{ MeV} \tag{12}$$

in isospin symmetric pure QCD we are able to extract

$$\sqrt{t_0^{\text{phys}}} = \frac{\sqrt{t_0}f_{\pi K}}{f_{\pi K}^{\text{isoQCD}}} = 0.1443(7) \text{ fm} \quad (\chi\text{PT fit}, a < 0.08 \text{ fm}) \tag{13}$$

5

from the χPT fit. The isoQCD values in eq. (12) are obtained from the experimental decay rates of $\pi \rightarrow \ell\nu + \gamma$ and $K \rightarrow \ell\nu + \gamma$ by taking out the QED and isospin effects with the help of χPT . This introduces the largest (second) error, while the first error is due to the experimental decay rate, and the third is due to the uncertainty of the CKM matrix elements V_{ud} and V_{us}.

The physical scale t_0^{phys} enters in the beginning of the analysis to define the physical point $\left(\phi_2^{\text{phys}}, \phi_4^{\text{phys}}\right)$. We therefore find the fixpoint such that the resulting t_0^{phys} is the same one that is used in the definition of the physical ϕ_2 and ϕ_4. For the statistical error of this final result the full correlation of the errors between the various observables is taken into account. We find the physical point at

$$\phi_2^{\text{phys}} = 0.0779(7), \quad \phi_4^{\text{phys}} = 1.098(10). \tag{14}$$

The fact that we do not observe significant deviations from the fit formula does, of course, not mean that they are not present. To estimate this source of systematic error, we use a range of different extrapolations: the χPT formula has been substituted by a Taylor expansion in the quark masses around the symmetric point and we also augmented the continuum extrapolation by an $a^2 m_\pi^2$ term. Applying a series of cuts to the data by removing the coarsest lattices or the ones with larger pion masses, leads also to valid description of the data. All fits which we consider render a χ^2/dof between 1 and 2. Fits where the probability to find a χ^2 greater than the measured one is less than 5% are discarded. We then take the minimum and the maximum central values and use half their difference as our preliminary systematic error and arrive at

$$\sqrt{t_0^{\text{phys}}} = 0.1443(7)(13) \text{ fm}. \tag{15}$$

At present, the systematic error dominates.

4. Lattice Spacing

Having determined the intermediate scale t_0^{phys} at the physical point, we use it together with measurements for t_0/a^2 to calculate the lattice spacing a in physical units. Since measurements at the physical point are not available for all lattice spacings, we need to model the behavior of t_0 as a function of ϕ_2. Using next-to-leading order χPT [16] we arrive at the fit formula

$$R_{t_0}(\phi_2) = \frac{\sqrt{t_0}}{\sqrt{t_0^{\text{sym}}}} = \sqrt{1 + G\left(\phi_2 - \phi_2^{\text{sym}}\right)}. \tag{16}$$

The data along with the fit are shown in fig. 4. We see quite clearly that at $a = 0.085$ fm there are lattice artifacts which then disappear very quickly (more quickly than a^2). This phenomenon was also observed in fit 4. of Ref. [3]. We therefore perform a fit to the normalized scale $\sqrt{t_0/t_0^{\text{sym}}}$ leaving out the coarsest ensembles with $a = 0.085$ fm, as we have already done above. The figure is also good evidence for the smallness of mass-dependent a^2 effects. Further evidence is that the coefficients of mass-dependent cutoff effects in the Symanzik effective theory are very small for our discretization [17].
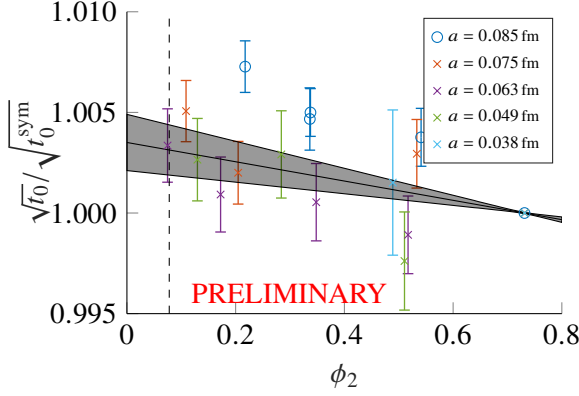
Figure 4: Scale $\sqrt{t_0}$ as a function of ϕ_2 normalized by the scale at the symmetric point for each lattice spacing. The fit includes all but the coarsest ensemble with $a = 0.085$ fm.

β	a [fm]
3.40	0.0849(5)(8)
3.46	0.0749(4)(7)
3.55	0.0633(4)(6)
3.70	0.0491(3)(4)
3.85	0.0385(2)(3)

Table 1: Lattice spacings a for each inverse coupling β with statistic and systematic errors.

The ratio $R_{t_0}(\phi_2^{\text{phys}})$ allows us to determine the scale t_0 in physical units at the symmetric point, $\sqrt{t_0^{\text{phys}}}$ where we can use the measured values for t_0/a^2 to extract the lattice spacing,

$$a = \frac{\sqrt{t_0^{\text{phys}}}}{R_{t_0}(\phi_2^{\text{phys}})} \cdot \frac{1}{\sqrt{t_0^{\text{sym}}/a^2}}. \tag{17}$$

Using eq. (15) we arrive at the lattice spacings listed in table 1.

5. Conclusion and Outlook

The scale setting method presented here is one of many choices. Using the pseudo-scalar decay constants has the advantage that they can be easily and precisely calculated on the lattice. Contaminations by excited state contributions can be thoroughly controlled. On the other hand our method is limited by the necessity to relate the experimental decay rates which include photons in the final state to the pure QCD decay constants as well as the dependency on the CKM matrix element V_{us}. The latter means in particular that the validity of the Standard model at low energies is assumed. However, the estimated uncertainties due to QED and the CKM matrix elements are still significantly below our overall precision and we are able to improve the result from the 2016 analysis [3]. Figure 5 compares the results from this analysis to previous determinations of $\sqrt{t_0}$ for $N_f = 2+1$ flavor and $N_f = 2+1+1$ flavor ensembles. It is worth noting that the central value of the previous CLS determination (labeled CLS 16) is more than 1σ above the current result. With the addition of several ensembles close to the physical point, it can now be seen that the point closest to the physical line in 2016 (purple point for $a = 0.063$ fm at $\phi_2 \approx 0.17$ in fig. 3) has a high statistical fluctuation upwards. This resulted in the previous analysis being skewed. It also highlights that precision scale setting, which is essential to precision results from lattice QCD, is a challenging endeavor. We need large statistics such that autocorrelations are under control as well as data at a large range of lattice spacings close to the continuum and quark masses sufficiently close to their
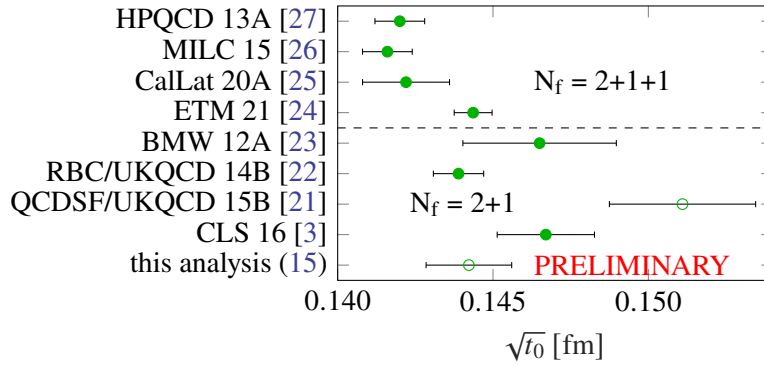
Figure 5: Comparison of $\sqrt{t_0}$ for different groups. Open symbols data points are not published.

physical values. Going significantly beyond the present accuracy will also require an improved control of isospin breaking and QED effects.

References

[1] M. Bruno et al., *Simulation of QCD with $N_f = 2 + 1$ flavors of non-perturbatively improved Wilson fermions*, *JHEP* **02** (2015) 043 [1411.3982].

[2] D. Mohler, S. Schaefer and J. Simeth, *CLS 2+1 flavor simulations at physical light- and strange-quark masses*, *EPJ Web Conf.* **175** (2018) 02010 [1712.04884].

[3] M. Bruno, T. Korzec and S. Schaefer, *Setting the scale for the CLS 2 + 1 flavor ensembles*, *Phys. Rev. D* **95** (2017) 074504 [1608.08900].

[4] M. Lüscher, *Properties and uses of the Wilson flow in lattice QCD*, *JHEP* **08** (2010) 071 [1006.4518].

[5] ALPHA collaboration, *QCD Coupling from a Nonperturbative Determination of the Three-Flavor Λ Parameter*, *Phys. Rev. Lett.* **119** (2017) 102001 [1706.03821].

[6] RQCD collaboration, *Masses and decay constants of the η and η' mesons from lattice QCD*, *JHEP* **08** (2021) 137 [2106.05398].

[7] RQCD collaboration, *Light-cone distribution amplitudes of octet baryons from lattice QCD*, *Eur. Phys. J. A* **55** (2019) 116 [1903.12590].

[8] RQCD collaboration, *Light-cone distribution amplitudes of pseudoscalar mesons from lattice QCD*, *JHEP* **08** (2019) 065 [1903.08038].

[9] RQCD collaboration, *Nucleon axial structure from lattice QCD*, *JHEP* **05** (2020) 126 [1911.13150].

[10] D. Djukanovic, T. Harris, G. von Hippel, P.M. Junnarkar, H.B. Meyer, D. Mohler et al., *Isovector electromagnetic form factors of the nucleon from lattice QCD and the proton radius puzzle*, *Phys. Rev. D* **103** (2021) 094522 [2102.07460].

[11] A. Gérardin, M. Cè, G. von Hippel, B. Hörz, H.B. Meyer, D. Mohler et al., *The leading hadronic contribution to* $(g - 2)_\mu$ *from lattice QCD with* $N_\mathrm{f} = 2 + 1$ *flavours of* $O(a)$ *improved Wilson quarks*, *Phys. Rev. D* **100** (2019) 014510 [1904.03120].

[12] D. Mohler and S. Schaefer, *Remarks on strange-quark simulations with Wilson fermions*, *Phys. Rev. D* **102** (2020) 074506 [2003.13359].

[13] A. Ramos and S. Sint, *Symanzik improvement of the gradient flow in lattice gauge theories*, *Eur. Phys. J. C* **76** (2016) 15 [1508.05552].

[14] J. Gasser and H. Leutwyler, *Light Quarks at Low Temperatures*, *Phys. Lett. B* **184** (1987) 83.

[15] J. Gasser and H. Leutwyler, *Chiral Perturbation Theory: Expansions in the Mass of the Strange Quark*, *Nucl. Phys. B* **250** (1985) 465.

[16] O. Bar and M. Golterman, *Chiral perturbation theory for gradient flow observables*, *Phys. Rev. D* **89** (2014) 034505 [1312.4999].

[17] N. Husung, P. Marquard and R. Sommer, *The asymptotic approach to the continuum of lattice QCD spectral observables*, 2111.02347.

[18] N. Husung, *Asymptotic behavior of cutoff effects of Gradient Flow observables in lattice Yang-Mills theory*, *in preparation* .

[19] Y. Aoki et al., *FLAG Review 2021*, 2111.09849.

[20] Particle Data Group collaboration, *Review of Particle Physics*, *PTEP* **2020** (2020) 083C01.

[21] V.G. Bornyakov et al., *Wilson flow and scale setting from lattice QCD*, 1508.05916.

[22] RBC, UKQCD collaboration, *Domain wall QCD with physical quark masses*, *Phys. Rev. D* **93** (2016) 074505 [1411.7017].

[23] S. Borsanyi et al., *High-precision scale setting in lattice QCD*, *JHEP* **09** (2012) 010 [1203.4469].

[24] EXTENDED TWISTED MASS collaboration, *Ratio of kaon and pion leptonic decay constants with Nf=2+1+1 Wilson-clover twisted-mass fermions*, *Phys. Rev. D* **104** (2021) 074520 [2104.06747].

[25] N. Miller et al., *Scale setting the Möbius domain wall fermion on gradient-flowed HISQ action using the omega baryon mass and the gradient-flow scales t_0 and w_0*, *Phys. Rev. D* **103** (2021) 054511 [2011.12166].

[26] MILC collaboration, *Gradient flow and scale setting on MILC HISQ ensembles*, *Phys. Rev. D* **93** (2016) 094510 [1503.02769].

[27] R.J. Dowdall, C.T.H. Davies, G.P. Lepage and C. McNeile, *V_{us} from π and K decay constants in full lattice QCD with physical u, d, s and c quarks*, *Phys. Rev. D* **88** (2013) 074504 [1303.1670].